Electronic structure and structural stability of the high-pressure orthorhombic phase of selenium

2001 J. Phys.: Condens. Matter 13 9401

(http://iopscience.iop.org/0953-8984/13/42/301)

INSTITUTE OF PHYSICS PUBLISHING JOURNAL OF PHYSICS: CONDENSED MATTER

J. Phys.: Condens. Matter **13** (2001) 9401–9410 PII: S0953-8984(01)25870-6

Electronic structure and structural stability of the high-pressure orthorhombic phase of selenium

Masaaki Geshi[1], **Tatsuki Oda and Yasuaki Hiwatari**

Department of Computational Science, Faculty of Science, Kanazawa University,
Kanazawa 920-1192, Japan

Received 18 June 2001, in final form 4 September 2001
Published 5 October 2001

Abstract

Electronic and atomic structures for high-pressure orthorhombic selenium were studied with first-principles calculations. Structural optimizations for four atoms in the orthorhombic unit cell were performed and the space group of the optimized structure was determined as $P2_1/m$, which is a monoclinic space group. The atomic structure optimized and the space group determined are consistent with the result of the x-ray diffraction measurement. The electronic density of states of the optimized structure is quite similar to that of the structure in the next high-pressure phase. This fact corresponds well to the experimental result that the transition to the next phase is a second-order one.

(Some figures in this article are in colour only in the electronic version)

1. Introduction

It is difficult to determine the space group for a given complex crystal due to ambiguity of atomic positions in a unit cell. Even when the Rietveld refinement is used, there may be some errors or some uncertainties. Sometimes, the quality of the measured data may be insufficient to allow us to obtain the atomic positions in the unit cell. In this work, we determine the space group of a high-pressure phase of selenium (Se) with a help of first-principles atomic force calculations.

When an electronic structure calculation for a crystal is performed, symmetry operations of a space group are usually used to reduce the computational burden. The assumed space group sometimes restricts the atomic position to a fixed site and thus influences the resulting electronic structure.

The structure of the fourth phase of Se under high-pressure (Se-IV) was reported from an experiment [1] to be an orthorhombic structure, which is identified from diffraction patterns and from the angle between the crystal axes in the x-ray experiments. However, the four atomic

---

[1] Present address: Steacie Institute for Molecular Science, National Research Council of Canada, 100 Sussex Drive, Ottawa, Ontario, Canada K1A 0R6.

positions in the unit cell have not been definitely determined yet. Therefore, the space group of the phase has not been identified, so far.

The electronic structure calculation for the orthorhombic structure was performed by Nishikawa *et al* [2] via a pseudopotential method. They adopted the space group[2] $Cmcm$ (D_{2h}^{17}) for the Se-IV phase following the suggestion based on the experiment that the Se-IV phase was base-centred orthorhombic (bco). They found that the bco structure has a higher energy for a particular volume than a β-Po-type rhombohedral structure of the next higher-pressure phase. It is also found that the density of states (DOS) for the bco structure has a deep dip just below the Fermi level on a sharp peak. These results imply that the atomic structure assumed in their calculation is invalid. Then they also calculated the electronic structure for the Se-IV phase by using another type of atomic structure. However, they did not find any valid electronic structure.

In the x-ray diffraction experiment of Akahama *et al* [1], there were twelve diffraction lines found in a diffraction window of $2\theta = 34^\circ$ for the Se-IV phase. With increasing pressure the number of diffraction lines was decreased down to four, with changes from doublets to singlets and decaying intensity. At the transition point, no clear discontinuous change of volume was observed within their experiment. They suggested that the transition to the next higher-pressure phase is of second order.

If this suggestion is true, the structure of the Se-IV phase should be related to the β-Po-type structure and the former should smoothly change to the latter at the transition point. Moreover, it is considered that the electronic structure of the Se-IV phase should be similar to that of the β-Po-type structure.

We have previously investigated electronic structures for a monoclinic structure (Se-II) [3], the β-Po-type structure (Se-V), and a bcc structure (Se-VI) [4,5]. A normal electronic structure, as opposed to the dip in the DOS below the Fermi level, has been observed in these phases. In the present work we have performed first-principles electronic structure calculations for the Se-IV phase and structural optimizations of the four atoms in the unit cell. Consequently, we have determined the space group of the phase and have examined in detail the origin of the dip below the Fermi level. We have also discussed the relations between the atomic positions and the electronic states.

2. Computational details

A full-potential linearized augmented-plane-wave (FLAPW) method was used to calculate the electronic structure and the force acting on the atoms. The calculation was carried out with the WIEN97 code [6]. The self-consistent potentials and charge densities were treated essentially with no shape approximation such as a muffin-tin potential. We employed the generalized gradient approximation (GGA) developed by Perdew, Burke and Ernzerhof [7]. We took electrons in $[\mathrm{Ar}](3\mathrm{d})^{10}$ states as core electrons; these were treated as relaxed. The muffin-tin radius of 2.0 au was used. The energy cut-off of 16 Ryd was taken to construct the basis of augmented plane waves. For the charge-density calculation in the self-consistent loop, 420 $\boldsymbol{k}$-points were sampled for a rough optimization of atomic positions and the number of $\boldsymbol{k}$-points was increased up to 1824 $\boldsymbol{k}$-points for the final optimization to evaluate the densities of states (DOSs) for the structure of the Se-IV phase. Structural internal parameters were optimized using atomic forces as a guide.

---

[2] In the paper of Nishikawa *et al* [2] the space group was not described clearly. However, in view of the atomic positions that they indicated, we regard the space group as $Cmcm$.

3. Results

The space group of the Se-IV phase has not been definitely determined yet on the basis of the experiment [1]; however, a crude crystal structure has been suggested, namely the bco structure shown in figure 1. Nishikawa *et al* used the space group for the phase, $Cmcm$ (D_{2h}^{17}), in which the atomic positions are represented by $(0, \pm\nu, \pm1/4)$, $(1/2, \pm\nu + 1/2, \pm1/4)$ with an internal parameter $\nu = 0.125$ [2]. Following their work, first we adopted the space group $Cmcm$ and optimized the internal parameter ν. We used lattice constants obtained from the experiment [1], as listed in table 1. In this paper, we assumed orthorhombic unit cells, following the experimental result for the Se-IV phase [1]. The ν-parameter optimized at 34.9 GPa was 0.1239 (case 1), which is close to the value used in the previous work [2]. Figure 2 shows the total DOS at 34.9 GPa. This accords with the result of Nishikawa *et al* very well. There is again a very deep dip just below the Fermi level and the Fermi level is located near a sharp peak. These features of the DOS should indicate that the bco structure with the space group, $Cmcm$, is unstable from the viewpoint of the electronic structure. Such an unstable electronic structure is possibly caused by unsuitability of the atomic positions. In other words, the symmetry used in the calculation causes a frustration of the atomic system through the electronic structure. This kind of instability may be recognized as a mechanism related to the band Jahn–Teller effect. Secondly, we performed the optimization for internal parameters, assuming no symmetry of the point group with the orthorhombic unit cell whose dimensions are listed in table 1. The internal parameters optimized at 34.9 GPa are shown in table 2 (case 2).

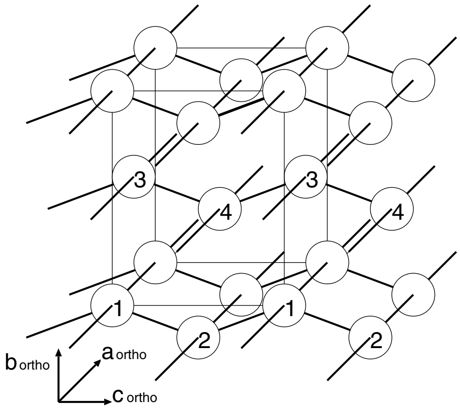

Figure 1. The orthorhombic structure suggested by the experiment [1] (case 1). The atomic positions are represented as $(0, \pm\nu, \pm1/4)$ and $(1/2, \pm\nu + 1/2, \pm1/4)$. In this space group, atoms $(\cdots 1–2–1 \cdots)$ and $(\cdots 3–4–3 \cdots)$ are in the respective b_{ortho}–c_{ortho} planes. Thin and thick lines indicate the orthorhombic frame and atomic bonds, respectively.

Table 1. The lattice constants used in this work for the Se-IV phase at three different pressures.

Pressure (GPa)	a (Å)	b (Å)	c (Å)
28.0	2.63	6.22	4.03
34.9	2.59	6.06	4.02
54.2	2.54	5.78	3.98

The total energy for case 2 is lower than that for case 1 by about 5.8 mRyd/atom, which is not small enough to be ignored. Figures 3 and 4 show the band dispersion and the total

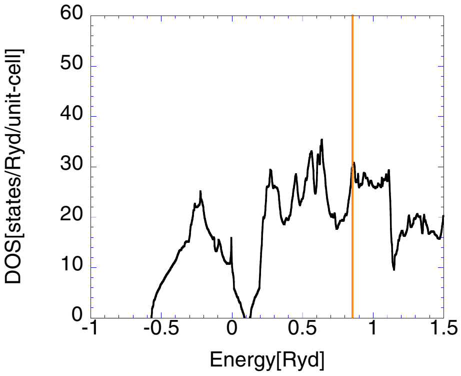

Figure 2. The DOS for case 1 (34.9 GPa). There is a deep dip just below the Fermi level (the vertical line).

Table 2. Atomic positions in the unit cell at 34.9 GPa with the space group *Cmcm* (case 1) and the result obtained when assuming no point group symmetry (case 2). The internal parameters were optimized.

	Case 1	Case 2
(x_1, y_1, z_1)	(0.0000, 0.1239, 0.2500)	(0.1234, 0.1251, 0.2501)
(x_2, y_2, z_2)	(0.0000, 0.8762, 0.7500)	(0.8769, 0.8749, 0.7498)
(x_3, y_3, z_3)	(0.5000, 0.6239, 0.2500)	(0.6260, 0.6251, 0.2506)
(x_4, y_4, z_4)	(0.5000, 0.3762, 0.7500)	(0.3737, 0.3752, 0.7495)

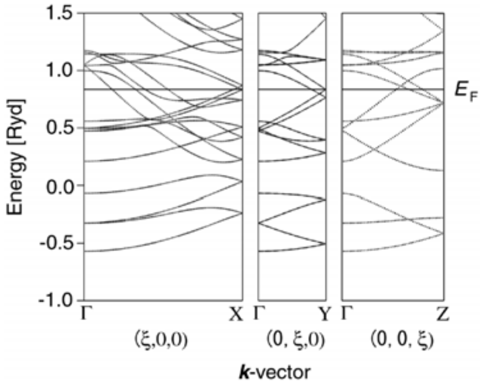

Figure 3. The band dispersion for case 2 (34.9 GPa).

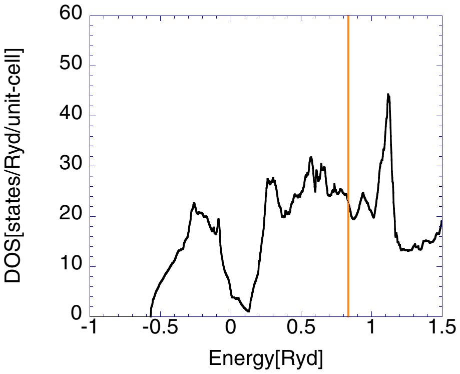

Figure 4. The DOS for case 2 (34.9 GPa). The deep dip below the Fermi level observed in figure 2 has completely disappeared.

DOS with the optimized atomic position at 34.9 GPa [1], respectively. In figure 3 there is a flat band just below the Fermi level in the vicinity of the X point on the Γ–X line. In figure 4 the deep dip which was present in case 1 has completely disappeared. From figures 2 and 4, the shapes of the two DOSs in the low-energy range (0.0–0.5 Ryd) are seen to be almost the same. However, the shapes around the Fermi level are quite different. The dip in figure 2 is filled by the states at or just above the Fermi level in case 1. It is considered that the difference in total energy is closely related to the change in the DOS around the Fermi level.

The difference in atomic positions between cases 1 and 2 is shown in figure 5. The maximum atomic displacement is about 0.33 Å along the a_{ortho}-axis, while the maximum displacements along the b_{ortho}-axis and c_{ortho}-axis are less than 0.01 Å. The most important difference between those atomic positions is the presence of a free internal parameter along the a_{ortho}-axis for case 2. When we calculated some different sets of internal parameters, which are free only along the directions of the b_{ortho}-axis and c_{ortho}-axis, the dip below the Fermi level was not filled out by our optimization. Therefore we conclude that the internal parameter (freedom) along the a_{ortho}-axis is fundamentally important for the electronic structure of the Se-IV phase. Indeed, it was found that the change for the DOS around the Fermi level comes from the change of the dispersion around the X point in the vicinity of the Fermi level.

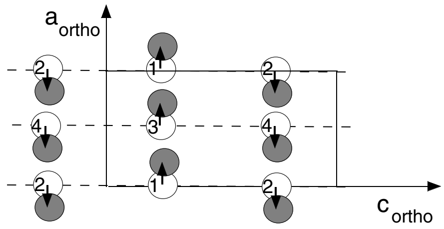

Figure 5. The difference in atomic positions between case 1 and case 2. Shaded circles indicate atoms of case 2. Arrows indicate displacements of atoms for case 1 to case 2.

Let us consider a valid space group for the Se-IV phase. From our optimized set of internal parameters, we interpreted the four atomic positions as $(x, y, 1/4)$, $(-x, -y, 3/4)$, $(x + 1/2, y + 1/2, 1/4)$, and $(-x + 1/2, -y + 1/2, 3/4)$ with $x = y = 1/8$. Note that the last two atoms are shifted from the first two atoms by $(1/2, 1/2, 0)$. Finally, from the existence of the mirror plane perpendicular to the c_{ortho}-axis on each atom and the screw axis along the c_{ortho}-axis through the centre of the nearest neighbours, we find the only valid space group to be $P2_1/m$ (C_{2h}^2) [8]. Then, the atomic positions are arranged at a pair of 2e Wyckoff positions. The details of the process used to determine the new space group are described in appendix A. It is a monoclinic space group and is one of the subgroups of the space group $Cmcm$. Although a monoclinic system does not usually need to have all three angles between the axes equal to 90°, in this case the angle between the a_{ortho}-axis and b_{ortho}-axis, γ, becomes by chance almost 90°.

We have checked whether the point with $x = y = 1/8$ provides the lowest energy. Total-energy calculations were performed for several sets of (x, y). It was verified that the lowest-energy point is located at this position. Total energies as a function of internal parameter x (y) at 34.9 GPa are shown in figure 6, where the other parameter y (x) is fixed at 0.125. From the variation with respect to the internal parameter x, we deduce that there is no large energy barrier between the space groups $Cmcm$ and $P2_1/m$.

The total energies for both space groups, $Cmcm$ and $P2_1/m$, are shown in figure 7 with $y = 0.125$ and $x = y = 0.125$, respectively. At each pressure the total energy for the $P2_1/m$ space group is at least 5 mRyd/atom lower than that for $Cmcm$. This value corresponds to a temperature much higher than that of the experiment [1]. These differences in total energy in the pressure range of interest ensure the stability of the structure for the $P2_1/m$ space group.

The space group $P2_1/m$ is consistent with the experimental result [1] because the configuration of four atoms is the same as those of the bco structure and therefore the reflection condition is the same. This is also true for the case of $\gamma = 90°$. In general, a monoclinic space group may not be consistent with the rules for orthorhombic space groups. However, the

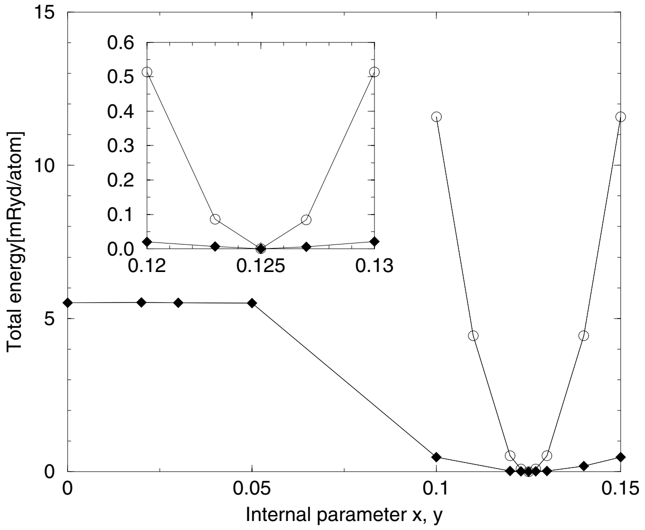

Figure 6. Total energy as a function of internal parameters, x and y, at 34.9 GPa. Diamonds and circles indicate the calculated values of x and y, respectively. The corresponding parameters, y and x, are fixed at 0.125, respectively.

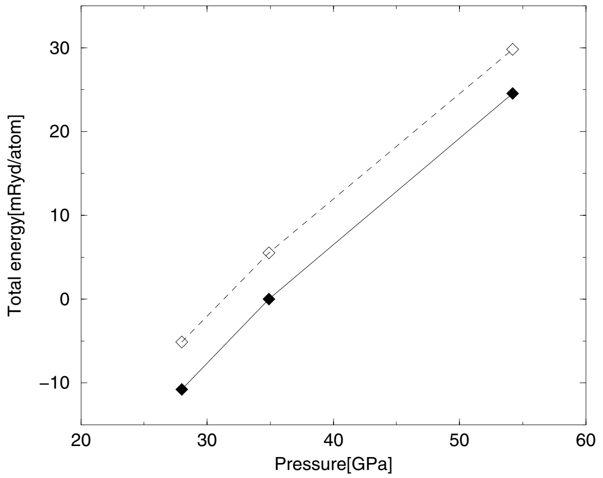

Figure 7. The total energies for both space groups, $Cmcm$ and $P2_1/m$. Open and filled diamonds are for $Cmcm$ and $P2_1/m$, respectively. The internal parameters are $v = 0.125$ for $Cmcm$ and $x = y = 0.125$ for $P2_1/m$.

atomic positions for the pair of 2e sites separated by (1/2, 1/2, 0) satisfy the same extinction law as those for the bco space group.

The DOS at 54.2 GPa (14.6 Å^3) is shown in figure 8, compared with that of the β-Po-type rhombohedral structure at 64 GPa (14.3 Å^3). The latter pressure was estimated in our previous work [5]. The DOSs for the Se-IV phase and the β-Po-type structure resemble each other quite closely. This is indirect evidence of a second-order transition to the Se-V phase.

It is interesting to see the local coordination of atoms for the new space group. The bond lengths between atom 1 and atom 2 in figure 1 and bond angles defined by atoms 1–2–1 are

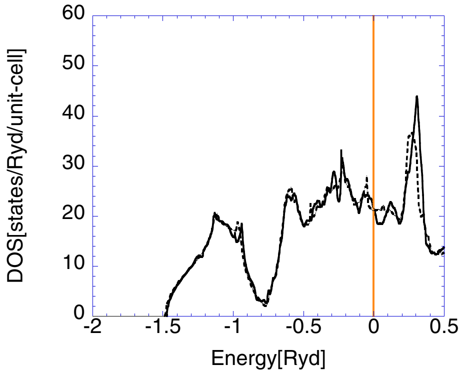

Figure 8. The total DOS at 54.2 GPa [1] and that of the β-Po-type structure at 64 GPa [4]. The former and the latter are shown by solid and dashed curves, respectively.

tabulated in tables 3 and 4. The bond lengths for space group $P2_1/m$ are longer than those for $Cmcm$ at all pressures. At 54.2 GPa, the bond length is reasonable, as compared to that of the β-Po-type rhombohedral structure as shown in figure 5 of reference [4], whereas the bond length for $Cmcm$ is much shorter than that of the β-Po-type structure. The bond angles for $P2_1/m$ are always smaller than those for $Cmcm$. The bond angle for $P2_1/m$ at 54.2 GPa is very close to the experimental rhombohedral angle of the β-Po-type structure, 104.2°, reported in figure 9(a) of reference [1]. The (1–2) length is almost the same as the atomic distance along the a_{ortho}-axis and the (1–4) length. This indicates that the coordination number of the atoms is six, although it was given as four in reference [1]. In the latter work, the atomic distance between atoms in two different neighbouring layers stacking along the b_{ortho}-axis was inferred to be longer from anisotropic compressibilities. However, the results of the present work indicate that the local coordination of atoms is already three dimensional in the Se-IV phase.

Table 3. The bond lengths and bond angles for $Cmcm$ and $P2_1/m$. The bond lengths are between atom 1 and atom 2 in figure 1.

Pressure (GPa)	$Cmcm$ (1–2) (Å)	(1–1) (Å)	(1–4) (Å)
28.0	2.55	2.63	2.86
34.9	2.52	2.58	2.83
54.2	2.46	2.54	2.77
Pressure (GPa)	$P2_1/m$ (1–2) (Å)	(1–1) (Å)	(1–4) (Å)
28.0	2.63	2.63	2.63
34.9	2.60	2.59	2.60
54.2	2.54	2.54	2.54

Table 4. The bond angles defined by atoms 1–2–1 in the c-direction. This angle corresponds to the rhombohedral angle of the β-Po-type structure.

Pressure (GPa)	$Cmcm$ (deg)	$P2_1/m$ (deg)
28.0	104.9	100.1
34.9	105.0	101.3
54.2	108.0	103.3

4. Discussion

The steep dip in the DOS for case 1 is completely filled out by allowing a degree of freedom in the direction of the a_{ortho}-axis. This corresponds to a change of eigenvalues around the X point in $\boldsymbol{k}$-space. Alternatively, the main component of the electronic states in the vicinity of the Fermi level could be related to the atomic p orbitals. From the partial DOS for case 1 shown in figure 9(a), we see that the main component of the DOS above the Fermi level arises from anti-bonding p orbitals in the direction of the a_{ortho}-axis (p_a). Figure 9(b) shows that the p_a DOS above the Fermi level exhibits an obvious decrease. This indicates that the dip is caused by the constraint in the direction of the a_{ortho}-axis as long as the space group $Cmcm$ is adopted.

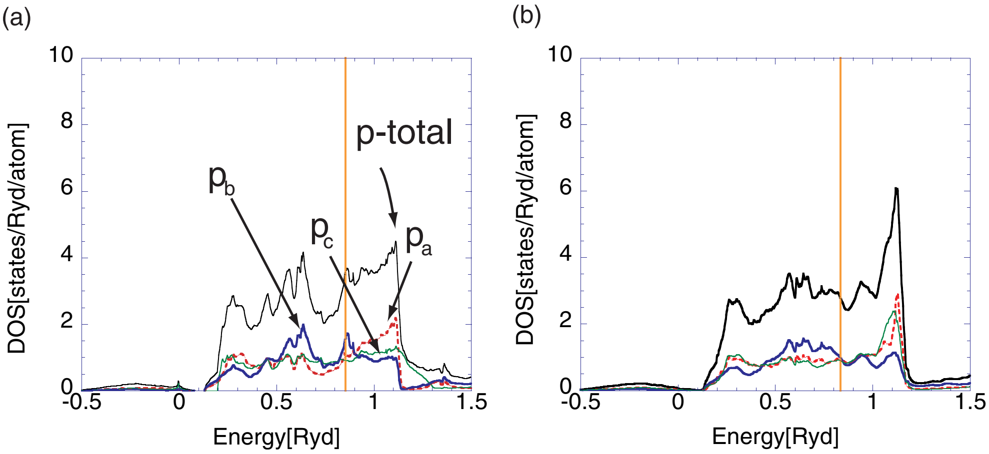

Figure 9. The partial DOSs of the p orbitals for (a) case 1 and (b) case 2. The change of p_a (the component in the a_{ortho}-direction) is remarkable.

If the transition to the β-Po-type structure is of second order, the structure represented by the space group $P2_1/m$ should be continuously transformed to the β-Po-type structure. Figure 10 shows the unit-vector correspondence between the orthorhombic and the rhombohedral frameworks. At the point of crossover between them we can represent the crystal axes of the rhombohedral structure, $\vec{a}_{\mathrm{r}}$, $\vec{b}_{\mathrm{r}}$, and $\vec{c}_{\mathrm{r}}$, in terms of $\vec{a}_{\mathrm{ortho}}$, $\vec{b}_{\mathrm{ortho}}$, and $\vec{c}_{\mathrm{ortho}}$ as follows:

$$\vec{a}_{\mathrm{r}} = -\vec{a}_{\mathrm{ortho}} \tag{1}$$

$$\vec{b}_{\mathrm{r}} = \frac{1}{4}\vec{a}_{\mathrm{ortho}} + \frac{1}{4}\vec{b}_{\mathrm{ortho}} + \frac{1}{2}\vec{c}_{\mathrm{ortho}} \tag{2}$$

$$\vec{c}_{\mathrm{r}} = \frac{1}{4}\vec{a}_{\mathrm{ortho}} + \frac{1}{4}\vec{b}_{\mathrm{ortho}} - \frac{1}{2}\vec{c}_{\mathrm{ortho}}. \tag{3}$$

From equations (1)–(3), the relations $\vec{a}_{\mathrm{ortho}} \cdot \vec{c}_{\mathrm{ortho}} = 0$, $\vec{b}_{\mathrm{ortho}} \cdot \vec{c}_{\mathrm{ortho}} = 0$ and $\vec{a}_{\mathrm{ortho}} \cdot \vec{b}_{\mathrm{ortho}} = -|\vec{a}_{\mathrm{r}}|^2(1 + 4\cos\alpha_{\mathrm{r}})$ are derived straightforwardly by assuming rhombohedral relations for $\vec{a}_{\mathrm{ortho}}$, $\vec{b}_{\mathrm{ortho}}$, and $\vec{c}_{\mathrm{ortho}}$, where α_{r} is a rhombohedral angle. Therefore, we obtain

$$\cos\gamma \equiv \frac{\vec{a}_{\mathrm{ortho}} \cdot \vec{b}_{\mathrm{ortho}}}{|\vec{a}_{\mathrm{ortho}}||\vec{b}_{\mathrm{ortho}}|} = -\frac{1 + 4\cos\alpha_{\mathrm{r}}}{\sqrt{9 + 16\cos\alpha_{\mathrm{r}}}}. \tag{4}$$

In reference [1] it is reported that α_{r} increases from 104.2° to 109.47° with increasing pressure in the β-Po phase. The former value of the angle α_{r} gives a γ of 89.5°, which is almost equal to 90°. We conclude that the transition could be of second order if the phase of the Se-IV is

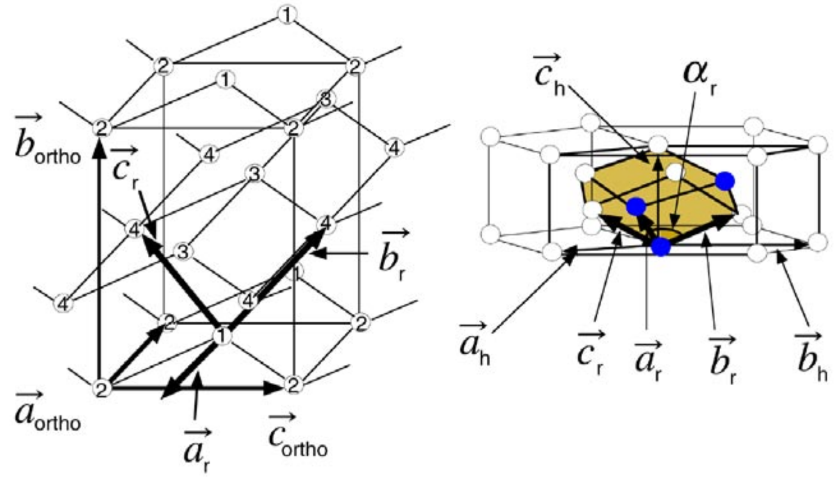

Figure 10. Correspondence between the orthorhombic and the β-Po-type rhombohedral structures.

the monoclinic phase satisfying equation (4). Although experiment indicates γ to be around 90° over the whole range of the Se-IV phase, it is not in general restricted for the space group $P2_1/m$.

Finally, working within the limitations of the present computational code, in order to check whether the angle γ is 90° or not, we have calculated total energies for several different angles γ around 90° at the fixed experimental volumes. The total energies have a minimum around 90°, which encourages us to believe that the conclusion in the present work would stand following optimization of the lattice constants.

5. Conclusions

In our first-principles calculation for the Se-IV phase the positions of four atoms in the orthorhombic frame and a particular space group, e.g. $P2_1/m$, have been obtained. The internal parameters x and y have been concluded to be 1/8 from our total-energy calculation. The total energies are at least 5 mRyd lower than that for $Cmcm$ over the whole pressure range of the phase. Our calculation presented in this work clearly showed an instability for the crystal structure with space group $Cmcm$ proposed on the basis of the previous calculation. The space group determined is consistent with the result of the x-ray diffraction measurement. The most important requirement for the space group is that there exists a free parameter in the direction of the $a_{\rm ortho}$-axis, which fundamentally affects the electronic structure near the Fermi level. From the resemblance of the DOSs and the correspondence of the unit vectors of the Se-IV and β-Po phases, it is concluded that the transition between the two phases is almost of second order.

In our preliminary calculations, a dip in the DOS just below the Fermi level like that for case 1 is also observed in the third phase of high-pressure Se (Se-III). From experiments [1,9] the structure of the Se-III phase is proposed to be of the same structure type as the monoclinic structure of high-pressure tellurium [10]. Recently the Se-III phase was also found to be unstable, from a first-principles calculation [11]. Although there have been crude analyses of the crystal structure for the Se-III phase, it will be necessary to approach stability conditions by means of structural studies based on electronic structure calculations.

Acknowledgments

We would like to thank Professor T Fujishita for discussions on space groups. We also acknowledge computational resources allocated by the Centre for Promotion of Computational Science and Engineering (CCSE) of Japan Atomic Energy Research Institute (JAERI). The calculation in this work was partially carried out using the facilities of the Supercomputer Centre, Institute for Solid State Physics, University of Tokyo. This work was financially supported by the Ministry of Education, Science, Sports and Culture.

Appendix A. Determination of the space group for the Se-IV phase

As shown above in table 2, we have determined the atomic positions of the Se-IV phase. These are represented as follows: $(x, y, 1/4)$, $(-x, -y, 3/4)$, $(x + 1/2, y + 1/2, 1/4)$, and $(-x + 1/2, -y + 1/2, 3/4)$. We can pick out two operations of the point group, which are a mirror operation in c_{ortho}-planes on each atomic site and a twofold screw rotation operation in the c_{ortho}-direction. However, there are no symmetry operations in the directions of the a_{ortho}- and b_{ortho}-axes. First, let us consider the structure of the Se-IV phase to be a bco structure or a primitive orthorhombic system [8]. In general, orthorhombic space groups must have some kind of twofold rotation operation for all axes orthogonal to each other. Therefore orthorhombic space groups are not appropriate. Secondly, we adopt monoclinic space groups to describe the structure of the Se-IV phase. For a monoclinic system there is a twofold rotation operation along the only axis. There are various possible space groups: Pm: $1a + 1b$; $P2/m$: $2n + 2m$; $P2_1/m$: $2e+2e$; and $C2/m$. $C2/m$ should be excluded because it does not have a mirror plane perpendicular to the c-axis when the c-axis is treated as a unique axis. $P2/m$ should also be excluded because the atomic positions are invalid. Pm is considered to be a lower-symmetry version of $P2_1/m$, since the former does not have the screw rotation operation axis. Therefore we conclude that the space group of the Se-IV phase is $P2_1/m$. The extinction law observed in the x-ray diffraction patterns is reproduced by the atomic positions of case 2.

References

[1] Akahama Y, Kobayashi M and Kawamura H 1993 *Phys. Rev.* B **47** 20
[2] Nishikawa A Niizeki K, Shindo K and Ohno K 1995 *J. Phys. Chem. Solids* **56** 551
[3] Geshi M, Oda T and Hiwatari Y 1999 *J. Phys. Soc. Japan* **68** 3341
[4] Geshi M, Oda T and Hiwatari Y 1998 *J. Phys. Soc. Japan* **67** 3141
[5] Geshi M, Oda T and Hiwatari Y 2000 *Prog. Theor. Phys. Suppl.* **138** 249
[6] Blaha P, Schwarz K and Luitz J 1999 *WIEN97, a Full Potential Linearized Augmented Plane Wave Package for Calculating Crystal Properties* Karlheinz Schwarz, Technical University of Vienna (ISBN 3-9501031-0-4)
This is an updated version of
Blaha P, Schwarz K, Sorantin P and Trickey S B 1990 *Comput. Phys. Commun.* **59** 399
[7] Perdew J P, Burke K and Ernzerhof M 1996 *Phys. Rev. Lett.* **77** 3865
[8] Hahn T 1996 *Space-Group Symmetry (International Tables for Crystallography vol A)* 4th revised edn (Dordrecht: Kluwer Academic)
[9] Ohmasa Y, Yamamoto I, Yao M and Endo H 1995 *J. Phys. Soc. Japan* **64** 4766
[10] Aoki K, Shimomura O and Minomura S 1980 *J. Phys. Soc. Japan* **48** 551
[11] Hsueh H C, Lee C C and Wang C W 2000 *Phys. Rev.* B **61** 3851